

Persistent spin current in anisotropic spin ring

Yin Cheng^{a,*}, You-Quan Li^a, Bin Chen^b

^aZhejiang Institute of Modern Physics, Zhejiang University, Hangzhou 310027, PR China

^bDepartment of Physics, Hangzhou Teacher's College, Hangzhou 310012, PR China

Received 21 October 2005; received in revised form 4 January 2006; accepted 19 January 2006

Available online 18 July 2006

Abstract

The persistent spin current in an anisotropic spin ring penetrated by a SU(2) flux is studied by the Schwinger–Boson mean-field approach. The anisotropy in spin coupling can facilitate the persistent spin current. Ground-state energy and excitation-energy gap are also studied. A peak of spin current occurs at the maximum value of the ground-state energy.

© 2006 Published by Elsevier B.V.

PACS: 75.10.Jm; 75.10.Pq; 72.25.–b

Keywords: Persistent spin current; Anisotropic; Mean-field approach

1. Introduction

Quantum coherence plays a central role in mesoscopic physics and the persistent current on mesoscopic rings threaded by a magnetic flux is particularly a sensitive probe for such coherence. Thus persistent electrical current in mesoscopic ring has been well studied experimentally [1–3] and theoretically [4–7]. Owing to recent interests in the spin-based electronics [8], the study on spin current becomes a remarkable topic [9–13]. Persistent spin current in the ferromagnetic Heisenberg ring was shown to occur in the presence of crown-shaped magnetic field [14]. It can also be driven by inhomogeneous electric fields [15] due to the Aharonov–Casher effect [16]. On the basis of spin-wave approach, the spin current in antiferromagnetic Heisenberg ring in inhomogeneous magnetic field has been investigated very recently [17]. It is well known that the electrical persistent current is a topological current induced by magnetic flux, U(1) flux. However, as far as we are aware, there is no thorough discussion on the persistent spin current in the anisotropic Heisenberg model brought about by a SU(2) flux.

In this paper, we study an anisotropic Heisenberg rings (XXZ model) penetrated by SU(2) flux. In Section 2, we apply the Schwinger–Boson approach to study the model. In Section 3 we calculate the excitation spectrum and evaluate the ground-state energy and energy gap. In Section 4, we evaluate the persistent spin current and discuss the effects caused by the anisotropy in the model. In Section 5, we give a summary of our main results.

2. Schwinger–Boson approach

We consider a spin ring with anisotropy penetrated by SU(2) flux [18]:

$$H = \sum_j^N \left[\frac{1}{2} (e^{i\phi/N} s_j^+ s_{j+1}^- + e^{-i\phi/N} s_j^- s_{j+1}^+) + \Delta s_j^z s_{j+1}^z \right] + \text{h.c.}, \quad (1)$$

where s_j^\pm denote the spin-flipping operators, s_j^z the z component of spin operators, $\phi = \Phi/\Phi_0$ with Φ and Φ_0 ($= hc/e$) the SU(2) flux and the flux quanta, respectively and N the lattice number. Anisotropy is characterized by the parameter Δ . It is known that $\Delta < -1$ corresponds to the ferromagnetic regime and $-1 < \Delta$ the anti-ferromagnetic regime. Unlike U(1) flux which is spin independent, the SU(2) flux appearing in Eq. (1) is spin dependent,

*Corresponding author. Tel./fax: +86 571 87953689.

E-mail address: ycheng@hbar.zju.edu.cn (Y. Cheng).

which is obtained by making a gauge transformation with opposite sign for spin-up and spin-down particles, respectively. It can be regarded as an extension of magnetic flux of Maxwell field to Yang–Mills field. The latter has been applied to formulate [12] the Rashba spin–orbit coupling which occurs in certain semiconductors. The Hamiltonian (1) with an additional constant Zeeman term can be mapped into an effect spin model with a rotating magnetic field [19]. The presence of a constant magnetic field was shown to shift the ground state [20].

In terms of Schwinger–Boson operators a_j and b_j which satisfy the Bose commutation relations $[a_i, a_j^\dagger] = \delta_{ij}$ and $[a_i, b_j] = 0$, the spin operators are given by

$$s_j^+ = a_j^\dagger b_j, \quad s_j^- = a_j b_j^\dagger, \quad s_j^z = \frac{1}{2}(a_j^\dagger a_j - b_j^\dagger b_j), \quad (2)$$

with a local constraint at every site j given by $a_j^\dagger a_j + b_j^\dagger b_j = 2S$ which means only $2S$ of the two Bosons can occupy each site.

Since the lattice is a bipartite lattice, we can make a unitary transformation $a_{j+1} \rightarrow -a_{j+1}$, $b_{j+1} \rightarrow b_{j+1}$ at each site of one sublattice. This brings about $s_{j+1}^\pm \rightarrow -s_{j+1}^\pm$ and $s_{j+1}^z \rightarrow s_{j+1}^z$. The XXZ Hamiltonian (1) takes the following form:

$$H = \frac{1}{2} \sum_j \left[\left(-e^{i\phi/N} a_j^\dagger b_j a_{j+1} b_{j+1}^\dagger - e^{-i\phi/N} a_j b_j^\dagger a_{j+1}^\dagger b_{j+1} \right) + \frac{\Delta}{2} \left(a_j^\dagger a_j a_{j+1}^\dagger a_{j+1} - a_j^\dagger a_j b_{j+1}^\dagger b_{j+1} - b_j^\dagger b_j a_{j+1}^\dagger a_{j+1} + b_j^\dagger b_j b_{j+1}^\dagger b_{j+1} \right) \right] + \text{h.c.} \quad (3)$$

To fulfill the constraint, we need to introduce a Lagrangian-multiplier field λ_i . Then a generalized Hamiltonian is obtained:

$$H = - \sum_j \left\{ \left[\frac{1-\Delta}{4} \mathcal{A}_{j,j+1}^\dagger \mathcal{A}_{j,j+1} + \frac{1+\Delta}{4} \mathcal{B}_{j,j+1}^\dagger \mathcal{B}_{j,j+1} \right] + \text{h.c.} \right\} + 2 \sum_j \lambda_i (a_j^\dagger a_j + b_j^\dagger b_j - 2S) + 2NS^2 + (1-\Delta)NS, \quad (4)$$

where

$$\mathcal{A}_{j,j+1}^\dagger = e^{-i\phi/2N} a_j a_{j+1}^\dagger + e^{i\phi/2N} b_j b_{j+1}^\dagger, \\ \mathcal{B}_{j,j+1}^\dagger = e^{i\phi/2N} a_j^\dagger b_{j+1}^\dagger + e^{-i\phi/2N} b_j^\dagger a_{j+1}^\dagger.$$

The isotropy limits $\Delta = \pm 1$ (i.e., anti- and ferromagnetic cases) without flux were considered in Ref. [21]. At the mean-field level, we can take the average value of the multiplier field $\langle \lambda_i \rangle = \lambda$ and make the bond operators $\langle \mathcal{A}_{j,j+1}^\dagger \rangle = A^*$ and $\langle \mathcal{B}_{j,j+1}^\dagger \rangle = B^*$ uniform and static. We hence obtain the mean-field Hamiltonian:

$$H_{\text{MF}} = - \sum_j \left\{ \left[\frac{1-\Delta}{4} (A^* \mathcal{A}_{j,j+1} + A \mathcal{A}_{j,j+1}^\dagger) + \frac{1+\Delta}{4} (B^* \mathcal{B}_{j,j+1} + B \mathcal{B}_{j,j+1}^\dagger) \right] + \text{h.c.} \right\}$$

$$+ 2\lambda \sum_j (a_j^\dagger a_j + b_j^\dagger b_j - 2S) + \frac{1-\Delta}{2} A^* A N \\ + \frac{1+\Delta}{2} B^* B + 2NS^2 + (1-\Delta)NS. \quad (5)$$

By making use of a Fourier transform $a_j = \sum_{\mathbf{k}} a_{\mathbf{k}} \exp(i\mathbf{k}r_j)$ where the summation \mathbf{k} runs over the first Brillouin zone, a four-component spinor

$$\Psi_{\mathbf{k}}^\dagger = (a_{\mathbf{k}}^\dagger, a_{\mathbf{k}}, b_{-\mathbf{k}}^\dagger, b_{-\mathbf{k}}) \quad (6)$$

can be introduced. We can write the mean-field Hamiltonian into a compact form in the momentum space:

$$H_{\text{MF}} = \sum_{\mathbf{k}} \left\{ \Psi_{\mathbf{k}}^\dagger \left[\lambda - 2 \cos \left(\mathbf{k} + \frac{\phi}{2N} \right) \mathcal{M} \right] \Psi_{\mathbf{k}} + \frac{1-\Delta}{2} A 2 \cos \left(\mathbf{k} + \frac{\phi}{2N} \right) \right\} + \varepsilon_0, \quad (7)$$

where

$$\varepsilon_0 = \frac{1-\Delta}{2} A^* A N + \frac{1+\Delta}{2} B^* B N + (1-\Delta)NS + 2NS^2 - 2\lambda N(2S+1)$$

and

$$\mathcal{M} = \begin{pmatrix} \frac{1-\Delta}{4} A^* & 0 & 0 & \frac{1+\Delta}{4} B \\ 0 & \frac{1-\Delta}{4} A & \frac{1+\Delta}{4} B^* & 0 \\ 0 & \frac{1+\Delta}{4} B & \frac{1-\Delta}{4} A^* & 0 \\ \frac{1+\Delta}{4} B^* & 0 & 0 & \frac{1-\Delta}{4} A \end{pmatrix}.$$

The Hermitian property of the Hamiltonian (7) enables us to obtain that $A = A^*$. Using a Bogoliubov transformation given by the following transformation matrix \mathcal{T} :

$$\mathcal{T} = \begin{pmatrix} u & 0 & 0 & v \\ 0 & u & v & 0 \\ 0 & v & u & 0 \\ v & 0 & 0 & u \end{pmatrix}, \quad (8)$$

we transform the original Bose operators $\{a_{\mathbf{k}}^\dagger, a_{\mathbf{k}}, b_{-\mathbf{k}}^\dagger, b_{-\mathbf{k}}\}$ to a set of new Bose operators, called quasi-particle creation/annihilation operators $\{\alpha_{\mathbf{k}}^\dagger, \alpha_{\mathbf{k}}, \beta_{\mathbf{k}}^\dagger, \beta_{\mathbf{k}}\}$:

$$\mathcal{T} \begin{pmatrix} a_{\mathbf{k}}^\dagger \\ a_{\mathbf{k}} \\ b_{-\mathbf{k}}^\dagger \\ b_{-\mathbf{k}} \end{pmatrix} = \begin{pmatrix} \alpha_{\mathbf{k}}^\dagger \\ \alpha_{\mathbf{k}} \\ \beta_{\mathbf{k}}^\dagger \\ \beta_{\mathbf{k}} \end{pmatrix}. \quad (9)$$

Then the Hamiltonian is diagonalized:

$$H_{\text{MF}} = \sum_{\mathbf{k}} \left[\omega_{\mathbf{k},\phi} (\alpha_{\mathbf{k}}^\dagger \alpha_{\mathbf{k}} + \beta_{\mathbf{k}}^\dagger \beta_{\mathbf{k}} + 1) + \frac{1-\Delta}{2} A 2 \cos \left(\mathbf{k} + \frac{\phi}{2N} \right) \right] + \varepsilon_0, \quad (10)$$

where the quasi-particle spectrum is

$$\omega_{\mathbf{k},\phi} = \sqrt{\left[\lambda - \frac{1-\Delta}{2}A \cos\left(\mathbf{k} + \frac{\phi}{2N}\right)\right]^2 - \left|\frac{1-\Delta}{2}B \cos\left(\mathbf{k} - \frac{\phi}{2N}\right)\right|^2}. \quad (11)$$

Thus the free energy is obtained

$$f = \frac{F_{\text{MF}}}{2N} = \int_{-\pi/2}^{\pi/2} \frac{d\mathbf{k}}{2\pi} \left[\frac{2}{\beta} \ln \left(2 \sinh \frac{\beta \omega_{\mathbf{k},\phi}}{2} \right) + \frac{1-\Delta}{2}A \cos\left(\mathbf{k} + \frac{\phi}{2N}\right) \right] + \frac{\varepsilon_0}{2N}, \quad (12)$$

where $\beta = 1/k_B T$ with k_B the Boltzmann constant and T the temperature. The mean-field self-consistent equations are obtained by minimizing the free energy, i.e., $\delta f/\delta A = 0$, $\delta f/\delta B = 0$, $\delta f/\delta \lambda = 0$, then the saddle-point equations are given by

$$\begin{aligned} & \frac{1-\Delta}{2} \left\{ A + \int_{-\pi/2}^{\pi/2} \frac{d\mathbf{k}}{2\pi} \left[1 - \frac{\lambda - \frac{1-\Delta}{2}A \cos\left(\mathbf{k} + \frac{\phi}{2N}\right)}{\omega_{\mathbf{k},\phi}} \omega_{\mathbf{k},\phi} \right. \right. \\ & \quad \left. \left. \times \coth\left(\frac{\beta \omega_{\mathbf{k},\phi}}{2}\right) \right] \cos\left(\mathbf{k} + \frac{\phi}{2N}\right) \right\} = 0, \\ & \frac{1+\Delta}{2} \left\{ 1 - \frac{1+\Delta}{2} \int_{-\pi/2}^{\pi/2} \frac{d\mathbf{k}}{2\pi} \left[\frac{|\cos\left(\mathbf{k} + \frac{\phi}{2N}\right)|^2}{\omega_{\mathbf{k},\phi}} \coth\left(\frac{\beta \omega_{\mathbf{k},\phi}}{2}\right) \right] \right\} \\ & = 0, \\ & (2S+1) - \int_{-\pi/2}^{\pi/2} \frac{d\mathbf{k}}{2\pi} \left[\frac{\lambda - \frac{1-\Delta}{2}A \cos\left(\mathbf{k} + \frac{\phi}{2N}\right)}{\omega_{\mathbf{k},\phi}} \coth\left(\frac{\beta \omega_{\mathbf{k},\phi}}{2}\right) \right] \\ & = 0, \end{aligned} \quad (13)$$

which determine the parameters A , B and the Lagrange multiplier (chemical potential) λ in Eqs. (11) and (12). These saddle point equations can be solved numerically.

3. The ground-state energy and energy gap

We consider $S = 1$ at $T = 0$ K with $N = 50$ sites. At zero temperature, the ground-state (GS) energy equals the free energy because there is no thermal fluctuation. When $T \rightarrow 0^+$, β tends to $+\infty$ which means $e^{-\beta \omega_{\mathbf{k},\phi}/2} \rightarrow 0^+$ ($\omega_{\mathbf{k},\phi}$ is finite). Thus in the first term of the free-energy equation (12), $\ln(2 \sinh \frac{\beta}{2} \omega_{\mathbf{k},\phi})$ reduces to $\omega_{\mathbf{k},\phi}$ and the free energy (i.e., ground-state energy per site at $T = 0$) becomes

$$E_{\text{GS}}(\phi) = \int_{-\pi/2}^{\pi/2} \frac{d\mathbf{k}}{2\pi} \left[\omega_{\mathbf{k},\phi} + \frac{1-\Delta}{2}A \cos\left(\mathbf{k} + \frac{\phi}{2N}\right) \right] + \frac{\varepsilon_0}{N}. \quad (14)$$

We plot the ground-state energy per site versus θ (here we set $\phi/N = \theta$) for $\Delta = 0.9$ in Fig. 1 (the left figure). Apparently, the ground-state energy has a sharp cusp at $\theta/2\pi = \pm 0.5$ whose magnitude is -0.9626 , which is higher than average value of the energy gap. The height of cusp peak raises while Δ decreases, which is shown in the Fig. 1 (the right figure). In other words, the more anisotropy of spin chain, the sharper cusp in the curve.

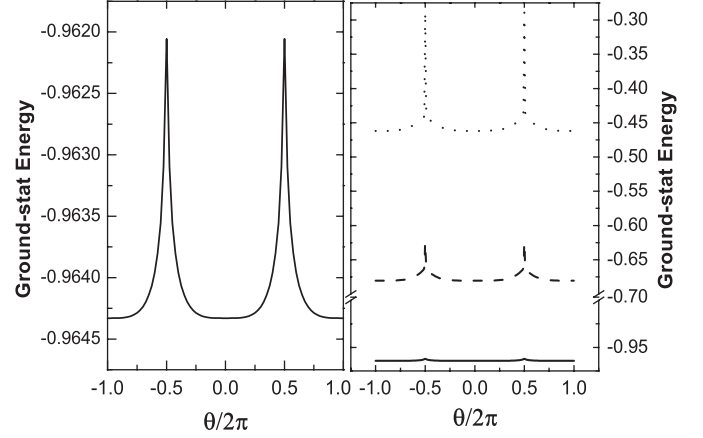


Fig. 1. The left figure is the ground-state energy versus SU(2) flux θ ($\theta = \phi/N$) for $\Delta = 0.9$. The right figure is that for various anisotropy $\Delta = 0.1$ (dot), $\Delta = 0.5$ (dash) and $\Delta = 0.9$ (solid) for comparison.

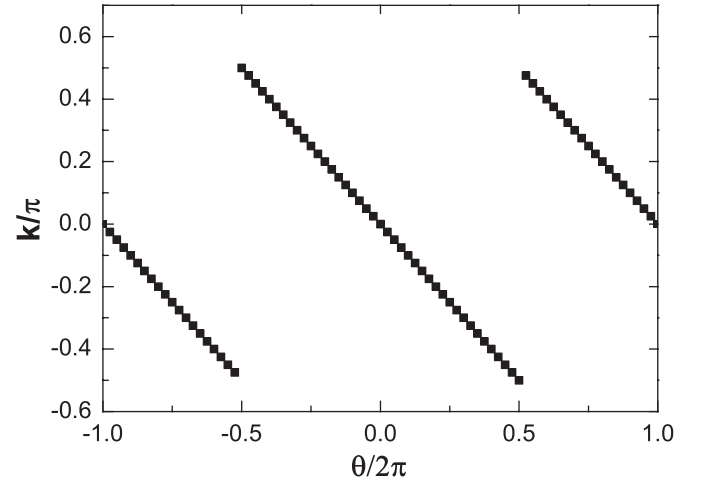


Fig. 2. Momentum versus flux for $\Delta = 0.9$.

We calculate the energy gap (EG) of the first excited state over the ground state. Unlike the usual case, the energy gap is not at $\mathbf{k} = 0$ due to the presence of the external SU(2) flux. This implies that the magnitude of the gap changes with the flux accordingly, which is shown in Fig. 2. Clearly, \mathbf{k} undergoes a jump at $\theta/2\pi = \pm 0.5$. Fig. 3 shows the excitation-energy gap versus the magnetic flux. The gap descends as the flux goes to $\theta/2\pi = \pm 0.5$, but rebounds when it is very close to $\theta/2\pi = \pm 0.5$ and reaches the maximum at $\theta/2\pi = \pm 0.5$.

4. Persistent spin current

We have previously obtained the ground-state energy and excitation spectrum whose values are determined by Eqs. (13). Now we are in the position to evaluate the persistent current at zero temperature ($T = 0$ K) which is defined by

$$I(\phi, T) = -\frac{\partial E_{\text{GS}}(\phi)}{\partial \phi}, \quad (15)$$

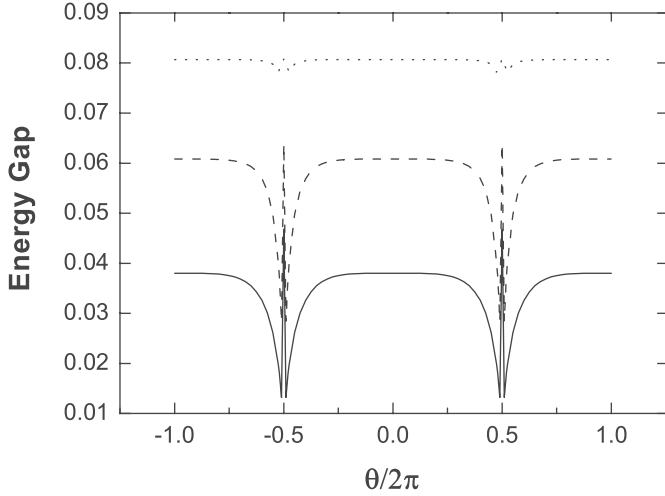
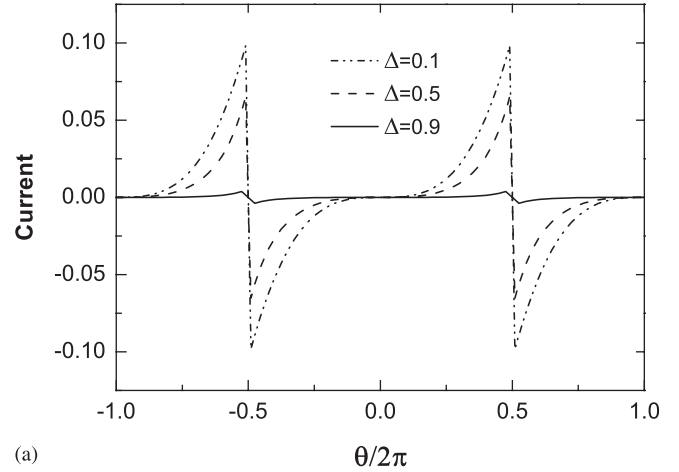
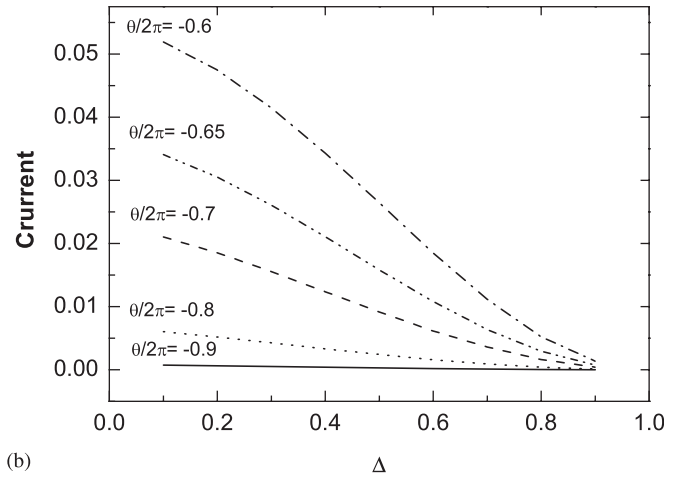


Fig. 3. The excitation energy gap versus flux for $\Delta = 0.1$ (solid), $\Delta = 0.5$ (dash) and $\Delta = 0.9$ (dot).



(a)



(b)

Fig. 4. (a) Persistent spin current versus flux for various anisotropy parameter Δ . The dash-dash-dash- and solid-line correspond to $\Delta = 0.1$, 0.5 and 0.9, respectively. (b) The current versus Δ illustrates the effects caused by anisotropy parameter.

where $E_{GS}(\phi)$ is the ground-state energy Eq. (14). The charge current I_c is null in our model for the particle is fixed on each site. However, the pure persistent spin current in the ring can be deduced by the SU(2) flux. We plot numerical calculation of Eq. (15) in Fig. 4(a). The jumps in the spin current curve occur at $\theta/2\pi = \pm 0.5$ for various Δ . We found that the anisotropy Δ will enhance the persistent spin current, which is shown in (b) of Fig. 4. As a result, the spin current in XY limit is larger than in Heisenberg limit. Fig. 5 exhibits that the energy gap decreases while persistent current increases. If the energy gap is larger, the spin flipping that contributes to spin current is prevented better.

5. Summary and discussion

Using Schwinger–Boson mean-field approach, we have investigated the property of ground-state and energy gap for the anisotropy spin ring penetrated by SU(2) flux. In the curve of energy versus flux (Fig. 1), there is a cusp at $\theta/2\pi = \pm 0.5$ and the energy reaches a maximum. The excitation-energy gap drops drastically nearby $\theta/2\pi = \pm 0.5$ but rebounds to maxima at $\theta/2\pi = \pm 0.5$. This implies that the energy curve of the first excited state has a similar shape as Fig. 1 and is tangent to the curve of the ground state near the point $\theta = \pm 0.5$. We calculated the pure persistent spin current and found that the flux dependence of persistent spin currents is facilitated by the anisotropy parameter Δ which promotes the persistent spin current, which is consistent with the conclusion of Ref. [19] by means of Bose-field approach. We also found that the peak of spin current appears at the minimal value of excitation gap. To justify the validity of mean-field approximation, we evaluated the aforementioned quantities by means of exact diagonalization of which all the features are qualitatively in agreement with our mean-field approach obtained in this paper.

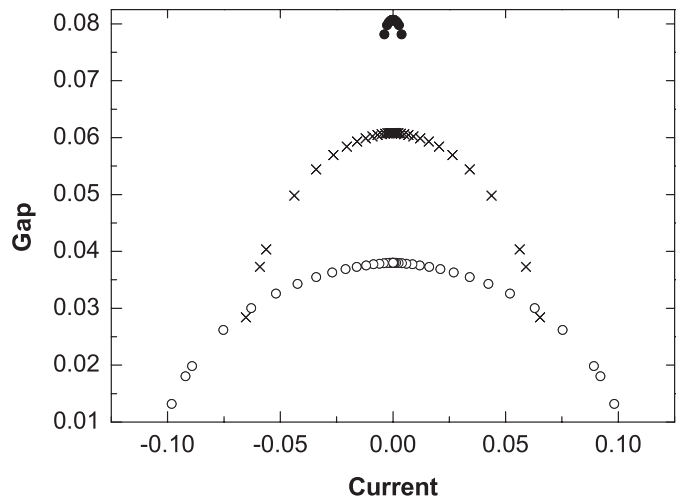


Fig. 5. Energy gap versus persistent spin current for different anisotropy parameters Δ . Hollow circle (o), cross (x) and solid circle (●) correspond to $\Delta = 0.1$, 0.5 and 0.9, respectively.

Acknowledgement

The work is supported by NSFC grant no. 10225419.

References

- [1] L.P. Levy, G. Dolan, J. Dunsmuir, H. Bouchiat, *Phys. Rev. Lett.* 64 (1990) 2074.
- [2] V. Chandrasekhar, R.A. Webb, M.J. Brady, M.B. Ketchen, W.J. Gallagher, A. Kleinsasser, *Phys. Rev. Lett.* 67 (1991) 3578.
- [3] D. Mailly, C. Chapelier, A. Benoit, *Phys. Rev. Lett.* 70 (1993) 2020.
- [4] M. Büttiker, Y. Imry, R. Landauer, *Phys. Lett. A* 96 (1983) 365.
- [5] V. Ambegaokar, U. Echern, *Phys. Rev. Lett.* 65 (1990) 381; U. Eckern, A. Schmid, *Europhys. Lett.* 18 (1992) 457.
- [6] Y.Q. Li, Z.S. Ma, *J. Phys. Soc. Japan* 65 (1996) 1519.
- [7] P. Koskinen, M. Manninen, *Phys. Rev. B* 68 (2003) 195304.
- [8] D. Awschalom, D. Loss, N. Samarth, *Semiconductor Spintronics and Quantum Computation*, Springer, New York, 2002.
- [9] S. Murakami, N. Nagaosa, S.C. Zhang, *Science* 301 (2003) 1348; S. Murakami, N. Nagaosa, S.C. Zhang, *Phys. Rev. B* 69 (2004) 235206.
- [10] J. Sinova, D. Culcer, Q. Niu, N.A. Sinitsyn, T. Jungwirth, A.H. MacDonald, *Phys. Rev. Lett.* 92 (2004) 126603.
- [11] E.G. Mishchenko, A.V. Shytov, B.I. Halperin, *Phys. Rev. Lett.* 93 (2004) 226602.
- [12] P.Q. Jin, Y.Q. Li, F.C. Zhang, *cond-mat/0502231*.
- [13] J. Splettstoesser, M. Governals, U. Zülicke, *Phys. Rev. B* 68 (2003) 165341.
- [14] F. Schütz, M. Kollar, P. Kopietz, *Phys. Rev. Lett.* 91 (2003) 017205.
- [15] Z.L. Cao, X.P. Yu, R.S. Han, *Phys. Rev. B* 56 (1997) 5077.
- [16] Y. Aharonov, A. Casher, *Phys. Rev. Lett.* 53 (1984) 319.
- [17] F. Schütz, M. Kollar, P. Kopietz, *Phys. Rev. B* 69 (2004) 035313.
- [18] G. Gavazzi, J. Wheatley, *Phys. Rev. B* 49 (1994) 13263.
- [19] D. Schmeltzer, A. Saxena, A.R. Bishop, D.L. Smith, *Phys. Rev. Lett.* 95 (2005) 066807.
- [20] P. Sun, D. Schmeltzer, *Phys. Rev. B* 61 (2000) 349.
- [21] Charles J. De Leone, Gergely T. Zimanyi, *Phys. Rev. B* 49 (1994) 1131.